Journal of Materials Chemistry B

Accepted Manuscript

ROYAL SOCIETY OF CHEMISTRY

www.rsc.org/materialsB

An injectable hydrogel formed by *in situ* cross-linking of glycol chitosan and multi-benzaldehyde functionalized PEG analogues for cartilage tissue engineering†

Luping Cao, Bin Cao, Chengjiao Lu, Guowei Wang, Lin Yu, Jiandong Ding*

State Key Laboratory of Molecular Engineering of Polymers, Department of Macromolecular Science, Fudan University, Shanghai 200433, China

* Corresponding authors, Tel: +86-21-65642531; fax: +86-21-65640293

E-mail address: yu_lin@fudan.edu.cn (L. Yu)

† Electronic Supplementary Information (ESI) available: Sequences of primers used for qRT-PCR.

Abstract: In this study, a muti-benzaldehyde functionalized poly(ethylene glycol) analogue, poly(ethylene oxide-*co*-glycidol)-CHO (poly(EO-*co*-Gly)-CHO), was designed and synthesized for the first time, and applied as a cross-linker to develop an injectable hydrogel system. Simply mixing two aqueous precursor solutions of glycol chitosan (GC) and poly(EO-*co*-Gly)-CHO led to the *in situ* formation of chemically cross-linked hydrogels under physiological conditions. The cross-linking was attributed to a Schiff's base reaction between amino groups of GC and aldehyde groups of poly(EO-*co*-Gly)-CHO. The gelation time, water uptake, mechanical properties and network morphology of the GC/poly(EO-*co*-Gly) hydrogels were well modulated by varying the concentration of poly(EO-*co*-Gly)-CHO. Degradation of the *in situ* formed hydrogels was confirmed both *in vitro* and *in vivo*. The integrity of the GC/poly(EO-*co*-Gly) hydrogels was maintained for up to 12 weeks subcutaneously in ICR mice. The feasibility of encapsulating chondrocytes in the GC/poly(EO-*co*-Gly) hydrogels was assessed. Live/Dead staining assay demonstrated that the chondrocytes were highly viable in the hydrogels, and no dedifferentiation of chondrocytes was observed after 2 weeks of *in vitro* culture. Cell counting kit-8 assay gave evidence of the remarkably sustained proliferation of the encapsulated chondrocytes. Maintenance of the chondrocyte phenotype was also confirmed with an examination of characteristic gene expression. These features suggest that GC/poly(EO-*co*-Gly) hydrogels hold potential as an artificial extracellular matrix for cartilage tissue engineering.

1. Introduction

Hydrogels are elastic three-dimensional polymeric networks that hold significant amounts of water yet retain their intact structures in water.[1-4] Because of their biomimetic nature and excellent biocompatibility, hydrogels have been extensively studied towards their applications in the pharmaceutical, biochemical, and other biomedically related fields.[5-15] In particular, injectable *in situ* formed hydrogels have gained increased attention as carriers for drug delivery, scaffolds for tissue engineering, etc.[16-26] Generally, such a system is a free-flowing fluid before injection and spontaneously turns into a semi-solid hydrogel once administered. Therapeutic drugs, bioactive factors or cells can be easily incorporated into the hydrogels by simply mixing them with precursor solutions, and then the precursor solutions can be injected into a defect site using minimally invasive procedures, followed by rapid formation of *in situ* hydrogels with any desired shape to match irregular defects.

Over the past decade, a variety of approaches have been investigated to fabricate injectable *in situ* formed hydrogels, including radical polymerization using redox or photo-initiators.[27, 28] It has been known that direct exposure to initiators and prolonged irradiation during polymerization led to poor cytocompatibility.[27, 28] Hence, it is vital for an injectable hydrogel system to cross-link under mild conditions. Recently, the Schiff's base reaction has become an attractive approach for preparing injectable hydrogels and has received much attention because the amino groups efficiently and orthogonally form imine bonds with aldehyde groups without any external stimulus

and extraneous reagents under physiological conditions.[29-32] To ensure cross-linking density within a three-dimensional network, precursor polymers with multiple functional amino and aldehyde groups are thus much required.

Chitosan is one of excellent choices for the Schiff's base linkages to form an injectable hydrogel due to the nature of abundant amino groups on the backbone, whereas the cross-linking agent with aldehyde groups became the bottleneck. Cross-linking of chitosan and its derivatives with small molecule dialdehydes, including glyoxal and glutaraldehyde to form hydrogels has been tried.[33] However, the toxicity of small molecule dialdehydes limits the biomedical applications for these hydrogel systems.[33] In recent years, many efforts have been made to develop multi-aldehyde functionalized macromolecular precursors, such as oxidized polysaccharides[34, 35] and difunctionalized poly(ethylene glycol) (PEG).[31] The use of strong oxidants effectively cleaves the vicinal glycols in polysaccharides to generate aldehyde groups but also causes undesired degradation of the polysaccharide backbone.[34, 36] Herein, we tried to design multi-aldehyde functionalized poly(ethylene glycol) (PEG) analogue as a new cross-linker. It is worthy of noting that dialdehyde PEG derivative as a cross-linker[31] has been reported to prepare chitosan hydrogel. We propose that multi-aldehyde functionalized PEG might be more efficient and exhibit higher tunability of gelation time *etc*. However, it is not available to obtain a linear PEG derivative with multiple aldehydes. Besides the possible choice to use star-like PEG, we tried to challenge an alternative route to obtain a linear PEG analogue with multiple aldehydes.

In the present study, we designed and synthesized a novel PEG analogue that possesses multiple aldehyde groups and then serves as a multifunctional cross-linker to react with amino groups of glycol chitosan (GC), a water-soluble chitosan derivate, to create injectable hydrogels, as schematically presented in Fig. 1. First, a random, linear polyether copolymer poly(ethylene oxide-*co*-glycidol) (poly(EO-*co*-Gly)) containing multiple pendent hydroxyl groups was successfully synthesized *via* a two-step reaction: (1) anionic copolymerization of 2,3-epoxypropyl-1-ethoxyethyl ether (EPEE) and ethylene oxide (EO), and (2) deprotection of the EPEE units. Considering that benzoic-imine bonds formed by aliphatic amines and aromatic aldehyde groups were more stable than imine bonds formed by aliphatic amines and aldehydes under physiological conditions,[29] benzaldehyde groups were chosen to modify the hydroxyl groups on the backbone of poly(EO-*co*-Gly) to form a multi-benzaldehyde functionalized poly(EO-*co*-Gly) (poly(EO-*co*-Gly)-CHO). By simply mixing two aqueous precursor solutions of GC and poly(EO-*co*-Gly)-CHO led to the *in situ* formation of chemically cross-linked hydrogels under physiological conditions. Physical properties including gelation time, gel content, water uptake, gel stiffness and morphology of the hydrogels were investigated, and their degradation *in vitro* and *in vivo* were detected and compared. Finally, the feasibility of encapsulating chondrocytes in the GC/poly(EO-*co*-Gly)-CHO hydrogels was assessed, and the viability, proliferation and phenotype reservation of *in situ* incorporated chondrocytes were examined.

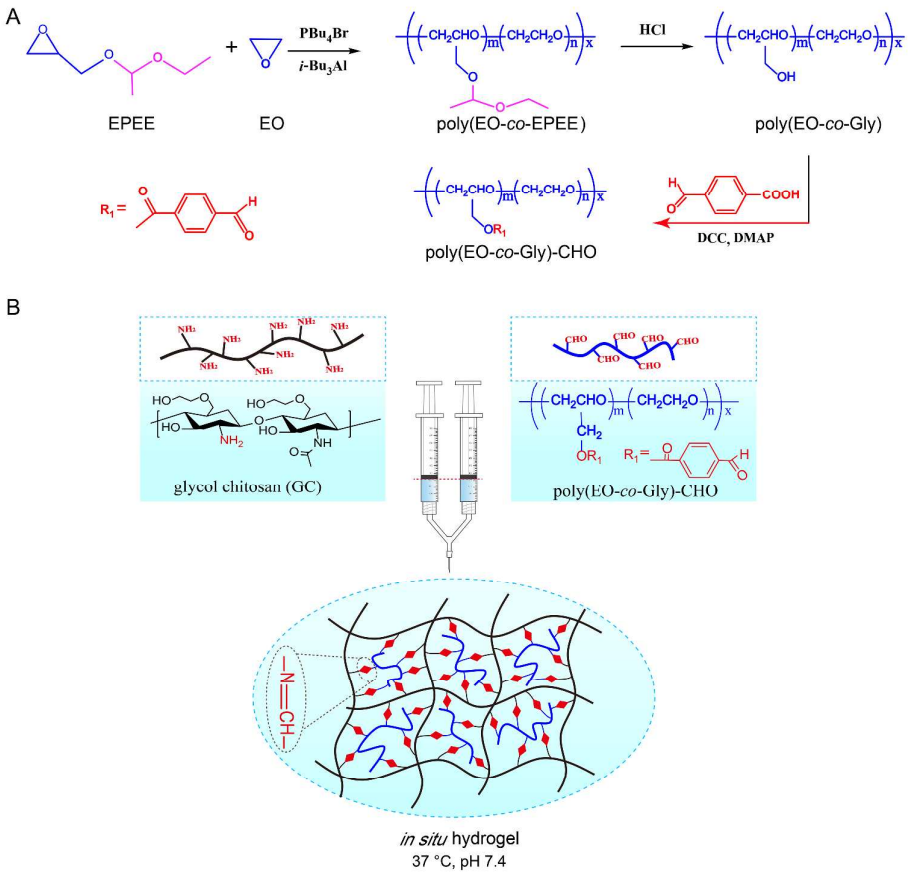

Fig. 1. (A) Molecular design of the multi-benzaldehyde functionalized PEG analogue, poly(EO-*co*-Gly)-CHO. (B) Schematic representation of the formation of injectable hydrogels chemically cross-linked by a Schiff's base reaction between aqueous solutions of GC and poly(EO-*co*-Gly)-CHO.

2. Materials and Methods

2.1 Materials

Triisobutylaluminum (*i*-Bu_3Al), 4-formylbenzoic acid, trichloroacetyl isocyanate (TAI), 4-(dimethylamino)pyridine (DMAP), *N,N′*-dicyclohexylcarbodiimide (DCC), GC (DP ≥400, purity ≥60%, degree of deacetylation of 90% as determined by

^{1}H-NMR in D_2O) and lysozyme obtained from chicken egg white (lot L6876) were obtained from Sigma-Aldrich (St. Louis, Missouri, USA). Tetrabutylphosphonium bromide (PBu_4Br) was purchased from Weifang Fine Chemicals Co., Ltd. Shanghai, China. EPEE was synthesized from glycidol and ethyl vinyl ether according to a literature procedure[37, 38] and distilled under reduced pressure. Other reagents were used without purification unless otherwise noted.

2.2 Synthesis of poly(ethylene oxide-*co*-2,3-epoxypropyl-1-ethoxyethyl ether) (poly(EO-*co*-EPEE)) and poly(EO-*co*-Gly)

Poly(EO-*co*-EPEE) was synthesized by random copolymerization of EPEE and EO using PBu_4Br as the initiator and *i*-Bu_3Al as the catalyst. Briefly, PBu_4Br (1.90 g in 100 mL toluene) was injected *via* a syringe into a vacuumed flame-dried ampoule in a dry ice/ethanol bath (-20 °C), and then 150 mL of toluene, 10.0 mL of EPEE and 13.5 mL of EO were introduced successively. After 10 min, 5.0 mL of *i*-Bu_3Al was added and the polymerization was performed with stirring at -20 °C for 24 h. The reaction was then terminated by the addition of 5.0 mL of methanol. After the removal of toluene using a rotary evaporator, the crude product was dissolved in CH_2Cl_2. The insoluble salts were removed by centrifugation, and the solution was concentrated and precipitated three times with diethyl ether. After vacuum drying at 45 °C for 48 h, the white powder was collected and stored at -20 °C until use.

Poly(EO-*co*-Gly) was obtained by hydrolysis of poly(EO-*co*-EPEE) using HCl as a hydrolytic reagent. For example, 2.0 g of poly(EO-*co*-EPEE) was mixed with 2.0 mL

of concentrated HCl (37%) and 10 mL of CH_3OH, and the mixture was stirred at room temperature for 3 h. The solvent was then removed *via* rotary evaporation and the crude product was purified by precipitating with CH_2Cl_2/diethyl ether. Finally, after drying under a vacuum at 45 °C for 24 h, the pale yellow product poly(EO-co-Gly) was obtained with a yield of 95%.

2.3 TAI derivatization of poly(EO-*co*-Gly)

Derivatization of poly(EO-*co*-Gly) with TAI was performed according to a previous publication with modifications.[39] Poly(EO-*co*-Gly) (100 mg) was dissolved in deuterochloroform ($CDCl_3$, 10 mL, dried by potassium carbonate and stored at dark place) in a 50-mL flask and an excess of TAI (200 μL) was added under an argon atmosphere. The reaction mixture was stirred for 24 h and then terminated by a few drops of D_2O. The mixture was filtered, and the solvent was then removed using a rotary evaporator. The resultant samples were dissolved in deionized water (20 mL), dialyzed (MWCO 3500 Da) against water and lyophilized to obtain a white powder.

2.4 Synthesis of poly(EO-*co*-Gly)-CHO

Poly(EO-*co*-Gly)-CHO was prepared *via* esterification between the hydroxymethyl groups of poly(EO-*co*-Gly) and the carboxyl group of 4-formylbenzoic acid. As is typical, poly(EO-*co*-Gly) (3.300 g, 3.20 mmol hydroxyl groups) was added to 100 mL toluene in a 250-mL Schlenk flask and the residual moisture in polymers was removed by azeotropic distillation of toluene to a volume of 15 mL. Then, anhydrous

dichloromethane (DCM, 50 mL), DMAP (97 mg, 0.80 mmol), DCC (2.641 g, 12.80 mmol) and 4-formylbenzoic acid (1.922 g, 12.80 mmol) were introduced successively. The reaction mixture was stirred under an argon atmosphere at room temperature for 48 h. Next, the solution was filtered, concentrated and precipitated with cold diethyl ether. The product obtained was collected by filtration and washed with cold diethyl ether. After drying under a vacuum at room temperature for 48 h, the product was dissolved in water and centrifuged (15000 r/min) for 20 min, and the supernatant was then lyophilized to obtain the final product (yield: 82%).

2.5 Characterization

^{1}H NMR spectra were obtained using an AVANCE III HD 400 MHz spectrometer (Bruker BioSpin International, Swiss) with $CDCl_3$ as the solvent and tetramethylsilane (TMS) as the internal reference. Molecular weights (MWs) and MW distributions of synthesized polymers were determined using a gel permeation chromatography system (GPC, Agilent 1260) equipped with a refractive index detector. Tetrahydrofuran (THF) was used as the eluting solvent at a flow rate of 1.0 mL/min at 35 °C, and the MWs were calculated based on narrowly dispersed polystyrene standards. Matrix assisted laser desorption ionization-time of flight mass spectrometry (MALDI-TOF MS) measurements were performed in a linear mode on an AB SCIEX TOF/TOF™ 5800 spectrometer (Applied Biosystems, USA). Ions were produced by irradiating the sample with a nitrogen laser (337 nm). *Trans*-2-[3-(4-*tert*-Butylphenyl)-2-methyl-2-propenylidene]malononitrile (DCTB) was chosen as the

matrix and sodium trifluoroacetate was chosen as the cationization agent. FT-IR spectroscopy analysis was performed on a Nicolet 6700 FTIR spectrometer (ThemoFisher, UAS) equipped with a DTGS detector. Each spectrum was recorded after 32 scans at a resolution of 4 cm^{-1}. The spectrum of lyophilized hydrogel was obtained using an attenuated total reflectance accessory (GladiART, Pike Technology). Other samples were prepared as a KBr pellet. All original spectra were baseline-corrected using OMNIC 8.2.387 software.

2.6 *In situ* hydrogel formation and gelation time determination

Two equivalent volumes of GC and poly(EO-co-Gly)-CHO solutions in phosphate buffer saline (PBS) were injected into a vial using a modified commercially available 3 mL 1:1 fibriJet® Applicator Assembly (Nordson Micromedics), which contains two syringes, one double cannulas blending connector, and one needle, as shown in Fig. 2. Then, the vials containing the precursor mixture solutions were incubated in a water bath at 37 °C and the gelation time was determined using a vial inverting method.[40, 41] No visible flow within 60 s was regarded as the criteria for gel formation when the vial was inverted vertically. All experiments were performed with four replicates.

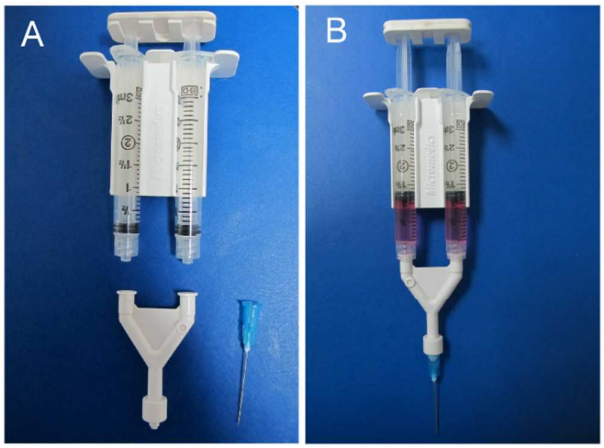

Fig. 2. The mixing device without (left) and with (right) precursor solutions. The device, which contains two syringes, one double blending connector, and one 23G needle, was modified from a 3-mL 1:1 fibriJet® Applicator Assembly. Equivalent volumes of precursor solutions were mixed thoroughly through a "Y" shape blending connector upon injection.

2.7 Gel content

Hydrogels (n = 4) were fabricated in vials according to the procedure described in Section 2.6. Twelve hours after gelation, samples were immersed in 5 mL of deionized water for 72 h and medium was replaced every 8 h to remove the salts and soluble polymers from the hydrogel samples. Next, hydrogels were lyophilized and weighed (W_{gel}). The gel content was defined as

$$\text{Gel content} = \frac{W_{gel}}{W_{GC} + W_{cross\text{-}linker}} \times 100\%$$

2.8 Water uptake

Hydrogel samples (n = 4) were prepared as described above and then immersed in PBS (5 mL) at an ambient temperature for 48 h. After removal of PBS, surface water on the hydrogels was carefully absorbed using facial tissue, and then the swollen hydrogels were weighed (W_{swollen}). Next, the samples were lyophilized to a constant weight (W_{dry}). The water uptake of hydrogels was calculated using the following equation:

$$\text{Water uptake} = \frac{W_{\text{swollen}}}{W_{\text{dry}}} \times 100\%$$

2.9 Rheological characterization

A Kinexus Pro rheometer (Malvern Instrument Inc., UK) equipped with a steel parallel-plate geometry of 40 mm in diameter was used to determine the rheological properties of the hydrogels. An amplitude sweep test was performed to determine the linear viscoelastic region (LVER) of *in situ* cross-linked hydrogels prior to time sweep test and frequency sweep test. All of the edges of the tested samples cured between parallel gaps (0.5 mm) were sealed with a minimum layer of dilute silicone oil to avoid the evaporation of water. All rheological tests were performed at 37 °C unless otherwise specified.

A time sweep test was carried out for 2 h to monitor gel formation kinetics. The storage modulus (G') and the loss modulus (G'') were recorded at a constant frequency of 1 Hz and strain of 1.0% as a function of time. Briefly, two precursor solutions with

a 1:1 volume ratio were injected on the center of the lower parallel plate through a modified 3-mL applicator assembly, and precursor solutions were allowed to cure at 37 °C.

For the frequency sweep test, samples were loaded using the same approach described above, and precursor solutions were incubated at 37 °C for at least 2 h to ensure complete gelation prior to performing the frequency sweep test. The strain was maintained at 1.0% in this test to ensure a LVER.

2.10 Hydrogel morphology

The cross-section morphology of *in situ* cross-linked hydrogels was examined with a scanning electron microscope (SEM, VEGA TS 5136MM, TESCAN). In a typical procedure, hydrogel specimens were immersed in liquid nitrogen, lyophilized, and then cut into thin sections using a sharp blade, followed by sputter-coating with gold. The cross-section morphologies were viewed using a SEM operated at an accelerating voltage of 10 kV.

2.11 Hydrogel degradation *in vitro*

Degradation of hydrogels *in vitro* was evaluated in the presence of enzyme according to a protocol published elsewhere.[11] Hydrogel samples (n = 4) were prepared in vials according to the procedure described in Section 2.6 and accurately weighed (W_0). Subsequently, 8 mL of PBS containing 1 mg/mL lysozyme and 0.02 wt% NaN_3 were added to the vials. Then, the vials were incubated in a shaking bath at

37 ℃ at a shaking rate of 50 rpm. The buffer was replaced twice per week during the first two weeks, and once a week thereafter. At predetermined time points, the buffer was removed, and the remaining hydrogels were carefully wiped using facial tissue to remove surface water and weighed (W_t). The weight ratio of the remaining hydrogel to original hydrogel, which is defined as $W_t / W_0 \times 100\%$, was monitored as a function of the degradation time.

2.12 Hydrogel degradation *in vivo*

ICR mice (20-23 g, SLAC Laboratory Animal Co. Ltd, Shanghai, China) were anesthetized by inhalation of diethyl ether. Then, 400 μL of hydrogel combined with 200 of μL GC (3.0 wt% in PBS) and 200 μL of multifunctional cross-linker poly(EO-*co*-Gly)-CHO (0.5 wt%, 1.0 wt%, and 4.0 wt% in PBS) were injected subcutaneously in the backs of ICR mice. All solutions were sterilized by filtration using 0.22-μm filters before administration. Some animals were sacrificed and dissected at scheduled intervals. Photographs of the remaining hydrogels were taken using a digital camera (Cannon S100V). All animal experiments were conducted in accordance with the "Principles of Laboratory Animal Care" (NIH publication #85-23, revised 1985) and approved by the ethics committee of Fudan University.

2.13 Chondrocyte isolation and culture

Chondrocytes were isolated from articular cartilage tissue from 7-day neonatal SD rats. The detailed procedure has been described in our previous publication.[42] The

isolated cells were cultured at 37 °C in a humidified atmosphere incubator containing 5% CO_2 and subcultured to passage 2 for follow-up experiments.

2.14 Encapsulation of chondrocytes in hydrogel

Solutions of GC (3.0 wt%) and poly(EO-*co*-Gly)-CHO (1.0 wt%) were prepared by dissolving the polymers in serum-free high-glucose DMEM containing 100 U/mL penicillin, 0.1 mg/mL streptomycin and 2 mM $_L$-glutamine. All solutions were sterilized by filtration using 0.22-μm filters prior to cell culture. Chondrocytes (passage 2) were suspended in a poly(EO-*co*-Gly)-CHO solution to form a cell suspension with a density of 100×10^5 cells/mL. Then, 100 μL of cell suspension was pipetted into a 24-well cell culture plate and mixed with 100 μL of GC solution by gentle agitation. Cell/hydrogel constructs were formed after incubation for 20 min. Then, 500 μL of high-glucose DMEM containing 10% FBS, 100 U/mL penicillin, 0.1 mg/mL streptomycin and 2 mM $_L$-glutamine was added gently onto the surfaces of the cell/hydrogel constructs and cultured at 37 °C in a humidified atmosphere incubator containing 5% CO_2. Culture medium was replaced every three days.

2.15 Cell viability assay

Chondrocytes within hydrogels were stained using a Live/Dead® Viability/Cytotoxicity Kit (Molecular Probe, USA). Chondrocytes/hydrogel constructs were incubated in PBS containing 2 μM Calcein AM and 1 μM ethidium homodimer-1 (EthD-1) for 40 min after 1, 7 and 14 days of culture. Samples were

visualized using a confocal laser scanning microscope (CLSM, LSM 710, Carl Zeiss) in a 24-well cell culture plate. Live cells were stained with Calcein AM (green) and dead cells were strained with EthD-1 (red).

2.16 Cell proliferation assay

A CCK-8 method was used to evaluate the proliferation of chondrocytes within hydrogels at 1, 7 and 14 days post-encapsulation according to the manufacturer's instructions. A solution of CCK-8 (500 μL, 10% v/v in high glucose DMEM culture media without phenol red) was added to each well of the plate, and the plate was incubated in a humidified atmosphere (37 °C, 5% CO_2). After 3 h of culture, 300 μL of media was transferred to a 96-well plate, and the absorbance at 450 nm was measured using a microplate reader (MultisKan MK3, Thermo Lab systems). The absorbance determined with hydrogels without chondrocytes was used as a blank.

2.17 RNA extraction and real-time quantitative polymerase chain reaction (qRT-PCR)

After dissolving the hydrogel/chondrocytes constructs with acetic acid (3 wt%, 500 μL/well), the total chondrocytes RNA released from the hydrogels was extracted using the MagneSil Total RNA miniIsolation System (Z3351, Promega) according to the manufacturer's instructions after culturing for 1, 7 and 14 days. RNA was dissolved in nuclease-free water and stored at -80 °C until use. The concentration and quality of extracted RNA was examined using a NanoDrop 2000 spectrometer

(Thermo Scientific). Total RNA (60 ng) was reverse-transcribed to cDNA using a PrimeScript RT reagent Kit (RR047A, Takara), according to the manufacturer's instructions. The qRT-PCR was conducted in a Rotor-Gene Q System (Qiagen) in combination with a Rotor-Gene SYBR Green PCR Kit (Qiagen), and standard recommended PCR protocols were performed as described elsewhere[42]. Relative expression of the gene of interest was normalized to GAPDH using the delta threshold cycle (Δt) method. The sequence of primers (Invitrogen) used for qRT-PCR is listed in Table S1 (See ESI).

2.18 Statistical analysis

All quantitative data are expressed as the mean ± standard deviation. Data for qRT-PCR from independent experiments (n = 3) were analyzed using the $2^{-\Delta\Delta Ct}$ method. Statistically significant differences in fold-changes in target gene expression were examined using a one-way analysis of variance (one-way ANOVA) with Fisher LSD significant difference test. A value of $p < 0.05$ was considered to be a statistically significant difference.

3. Results and discussion

3.1 Synthesis and characterization of poly(EO-*co*-Gly)-CHO

The random copolymer poly(EO-*co*-EPEE) was synthesized by anionic copolymerization of EPEE and EO using PBu_4Br as the initiator and *i*-Bu_3Al as the catalyst as presented in Fig. 1A. The ^{1}H-NMR spectrum of poly(EO-*co*-EPEE) is

shown in Fig. 3A. The peaks at δ 4.68-4.75 ppm, 1.28-1.33 ppm and 1.16-1.23 ppm were assigned to the methine proton (H_g), and methyl protons (H_f, H_i) of the EPEE unit, respectively. The signal of backbone (H_a, H_b, H_c, H_d) and lateral (H_e, H_h) protons occurred at δ 3.40-3.85 ppm. The molar ratio of EO/EPEE reads 28 as calculated from equation (1),

$$R = \frac{A_{\text{sum}} - 7A_{\text{g}}}{4A_{\text{g}}} \quad (1)$$

where R is the molar ratio of EO to EPEE unit, A_{sum} is the sum of integrals from δ 3.40 to 3.85 ppm, and A_{g} is the integral during δ 4.68-4.75 ppm.

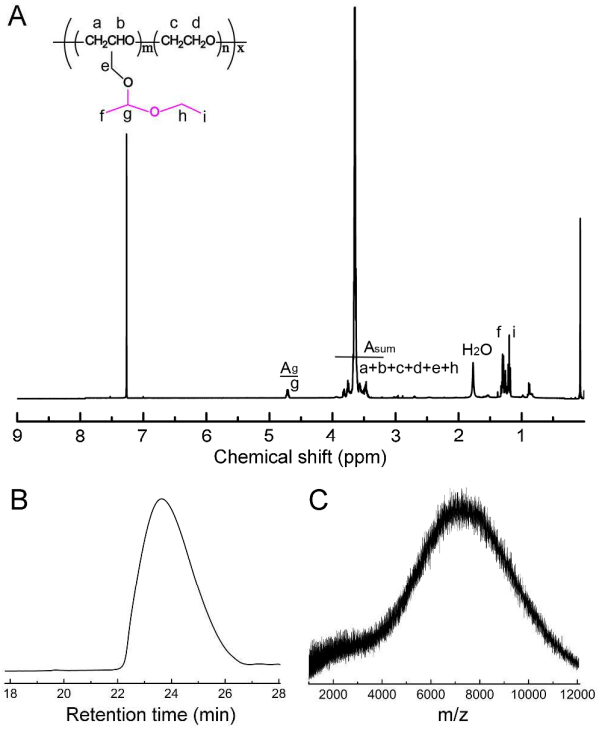

Fig. 3. (A) ^{1}H-NMR spectrum of poly(EO-*co*-EPEE) in $CDCl_3$; (B) GPC trace and (C) MALDI-TOF mass spectrum of poly(EO-*co*-EPEE).

Further, both the GPC trace (Fig. 3B) and the MALDI-TOF mass spectrum (Fig. 3C) of poly(EO-*co*-EPEE) show a unimodal MW distribution, indicating well-controlled

polymerization. The number-average molecular weight (M_n) and the molecular distribution of poly(EO-*co*-EPEE) determined by GPC analysis (M_n = 6800, M_w/M_n = 1.28) are slightly different from those determined by MALDI-TOF MS (M_n = 6600, M_w/M_n = 1.12). Because the MW determined by GPC is obtained from calibrations using narrowly dispersed linear polystyrenes, which are dramatically different both in molecular structure and chemical composition from poly(EO-*co*-EPEE), the MW (M_n = 6600) obtained from MALDI-TOF MS was used for subsequent feeding.

Deprotection of the EPEE units of poly(EO-*co*-EPEE) was performed in the presence of HCl in methanol, and the resulting polymer, poly(EO-*co*-Gly), was characterized *via* ^{1}H-NMR measurements (Fig. 4A). The result revealed the complete deprotection of the EPEE units, as shown by the disappearance of the methine signals at δ 4.7 ppm. Consequently, a linear multi-hydroxyl functionalized copolymer poly(EO-*co*-Gly) was obtained.

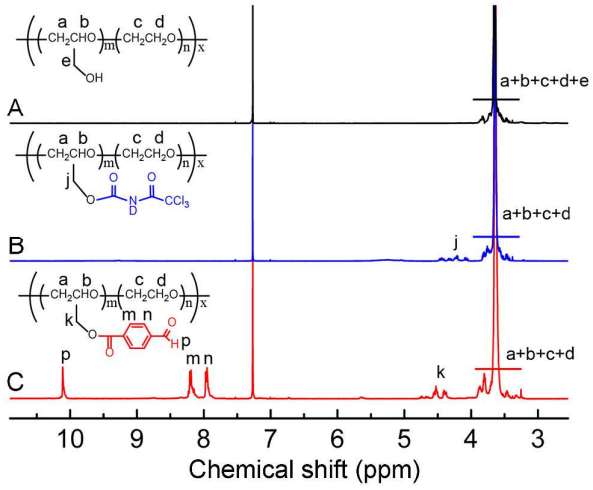

Fig. 4. ^{1}H-NMR spectra of (A) poly(EO-*co*-Gly), (B) TAI-capped poly(EO-*co*-Gly) and (C) poly(EO-*co*-Gly)-CHO in $CDCl_3$.

It is worth noting that the acid labile protecting units EPEE of poly(EO-*co*-EPEE) are susceptible to cleavage in solvents containing acidic moieties and it has been reported that the $CDCl_3$, a NMR solvent, will decompose and become acidic regardless of the storage container or conditions,[43] indicating that the EO/EPEE ratio calculated by its ^{1}H-NMR spectrum in $CDCl_3$ did not truly reflect the composition of poly(EO-*co*-EPEE). To determine the actual composition, we further used TAI, a commonly used derivatization agent for polymer end-group analysis,[39, 44] to quantitatively analyze the composition of poly(EO-*co*-Gly). The derivatization proceeded for 24 h to ensure that all hydroxyl groups became substituted with TAI, though it has been reported[39] that this reaction proceeds rapidly and is complete within 30 min at room temperature. The ^{1}H-NMR spectrum of TAI-capped poly(EO-*co*-Gly) is presented in Fig. 4B. The proton signals for imidic ($-CH_2CON\boldsymbol{H}COCl_3$) was almost undetectable due to H-D exchange upon the addition of D_2O. However, the signal for the α-methylene protons of $-C\boldsymbol{H_2}CONHCOCl_3$, which is suitable for quantitation, shifted from δ 3.4-3.9 ppm to δ 4.3-4.6 ppm, a clear region within the ^{1}H NMR spectrum of TAI-capped poly(EO-*co*-Gly). Comparing the integral of the α-methylene protons of $-C\boldsymbol{H_2}CONHCOCl_3$ with that of $-C\boldsymbol{H_2}C\boldsymbol{H_2}O-$ and $-C\boldsymbol{H_2}C\boldsymbol{H}O-$ on the backbone of poly(EO-*co*-Gly) appearing at δ 3.4-3.9 ppm, the molar ratio of EO/EPEE was 20, which was considered more reliable than the result obtained from the ^{1}H-NMR spectrum of poly(EO-*co*-EPEE) in $CDCl_3$ (Fig. 3A). Combining the MW of poly(EO-*co*-EPEE) (M_n = 6600) determined by MALDI-TOF

MS (Fig. 3C), we confirmed that each random copolymer poly(EO-*co*-Gly) chain possesses 6.4 hydroxymethyl groups on average.

Benzaldehyde functionalization of poly(EO-*co*-Gly) was accomplished by reacting the free hydroxymethyl groups with 4-formylbenzoic acid. ^{1}H-NMR analysis confirmed the successful introduction of benzaldehyde functional groups into poly(EO-*co*-Gly) with the appearance of the characteristic peak of -PhC***H***O at δ 10.10 ppm and aromatic protons peaks at 8.21 and 7.97 ppm (Fig. 4C). The extent of the conversion from hydroxyl groups to benzaldehyde groups was also calculated by comparing the integral of the α-methylene protons of -C$\boldsymbol{H_2}$COOR$_\mathbf{1}$ pendant groups of poly(EO-*co*-Gly)-CHO with that of -C$\boldsymbol{H_2}$C$\boldsymbol{H_2}$O- and -C$\boldsymbol{H_2}$C***H***O- on the backbone of poly(EO-*co*-Gly)-CHO appearing at δ 3.4-3.9 ppm. Almost complete substitution (98%) was obtained, demonstrating that the esterification reaction is highly efficient. In addition, the introduction of benzaldehyde groups did not influence the solubility of poly(EO-*co*-Gly)-CHO in water, which is very important for biomedical applications.

3.2 *In situ* gel formation, gelation time, gel content, and water uptake

GC and poly(EO-*co*-Gly)-CHO were dissolved in PBS (pH 7.4), and then loaded into separate syringes. Equivalent volumes of precursor solutions were thoroughly mixed through the "Y" shape connector upon injection, which then spontaneously formed transparent hydrogels under physiological conditions. The *in situ* formation of chemically cross-linked hydrogels was confirmed using FT-IR analysis, as illustrated

in Fig. 5. In the FT-IR spectrum of the GC/poly(EO-co-Gly) hydrogel, the absorption band at 1723 cm^{-1}, which is attributed to the benzaldehyde carbonyl of poly(EO-co-Gly)-CHO, all but disappeared. In contrast, this characteristic absorption was distinctly observed in the spectrum of the physical mixture of GC and poly(EO-*co*-Gly)-CHO powders. This finding indicates that the reaction between benzaldehyde and amino groups in aqueous solution proceeded with high efficiency and that essentially no benzaldehyde residue was retained, which is very important for ensuring the biocompatibility and safety of *in situ* formed hydrogels. The absorption peaks at 1654 cm^{-1} and 1596 cm^{-1}, which are assigned to the C=O stretching of amino acetyl groups and N-H bending of amino groups in GC,[45] respectively, were still observed in the GC/poly(EO-co-Gly) hydrogel, indicating the existence of excess free amino groups. These free amino groups provide the possibility for further biochemical labeling or other modifications.

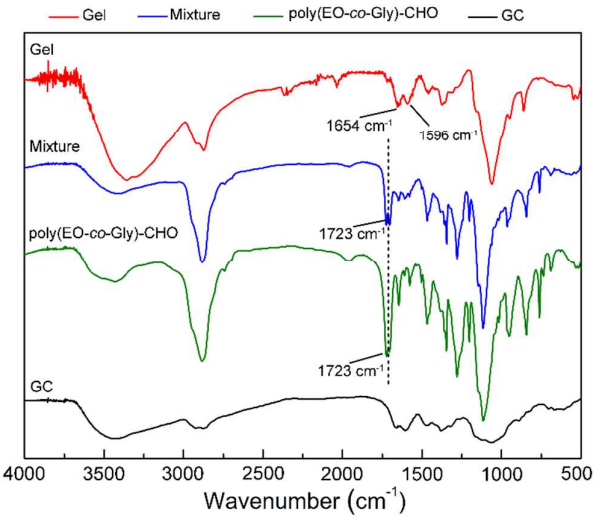

Fig. 5. FT-IR spectra of the lyophilized GC/poly(EO-*co*-Gly) hydrogel containing 1.5 wt% GC and 0.5 wt% poly(EO-*co*-Gly)-CHO, the physical mixture of GC and poly(EO-co-Gly)-CHO powders, poly(EO-*co*-Gly) and GC.

Fig. 6A displays the *in situ* formed GC/poly(EO-*co*-Gly) hydrogels in both PBS and DMEM medium, revealing good adaptability of the Schiff's base reaction. From the perspective of clinical administration, the gelation time of *in situ* formed hydrogels should be adjustable. A gelation time that is too short might not only block the needle during injection but could also cause a heterogeneous distribution of cells or drugs within the hydrogel matrix. On the other hand, too long of a gelation time would result in settling of the seeding cells at the bottom of the gels, and may raise the risk of leaking soluble factors, if present, and cells to surrounding tissues when administered *in situ*. To evaluate the influence of cross-linker concentration on gelation time, a series of concentrations of poly(EO-*co*-Gly)-CHO was used to fabricate *in situ* formed hydrogels, and the corresponding gelation time was determined *via* the vial inverting method. Increasing the cross-linker concentration from 0.25 wt% to 2.0 wt% at a given GC concentration resulted in a significant decrease in gelation time from 204 ± 3 s to 64 ± 8 s (Fig. 6B). It is obvious, then, that the gelation time decreases as the concentration of cross-linker increases.

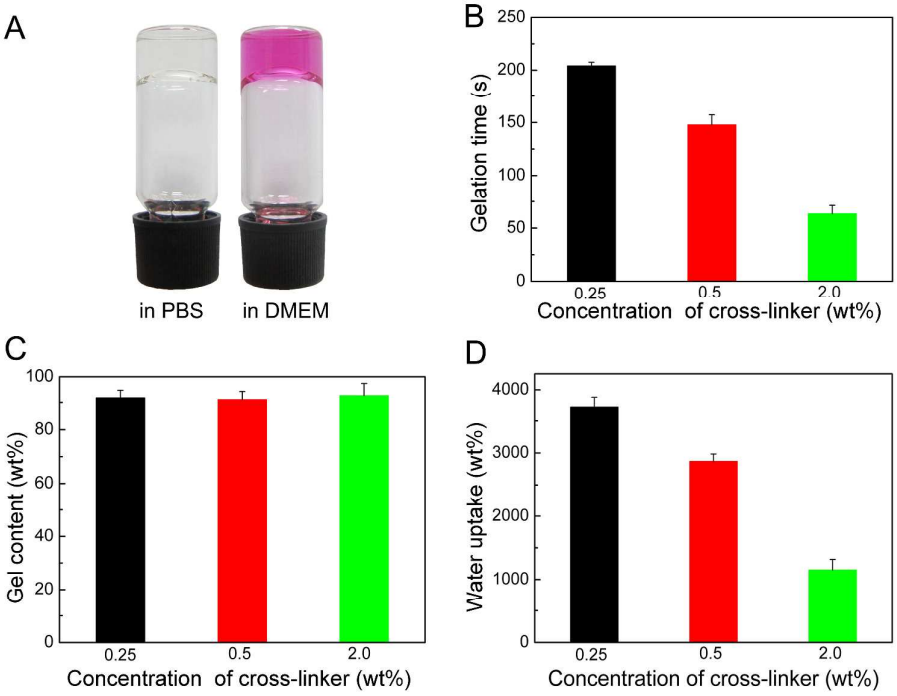

Fig. 6. (A) Gross views of the GC/Poly(EO-*co*-Gly) hydrogels in PBS and DMEM medium; (B-D) gelation time, gel content and water uptake of GC/Poly(EO-*co*-Gly) hydrogels in PBS as a function of the concentration of poly(EO-*co*-Gly)-CHO at 37 °C. The final concentration of GC in the hydrogel was fixed at 1.5 wt%. All experiments were performed with four replicates.

The gel content of GC/poly(EO-*co*-Gly) hydrogels was determined using the gravimetric method. Fig. 6C shows that the gel content was greater than 90% for all samples, demonstrating the efficiency of the Schiff's base reaction.

The water uptake of GC/poly(EO-*co*-Gly) hydrogels was also dependent on the concentration of poly(EO-*co*-Gly)-CHO, as shown in Fig. 6D. As the concentration of cross-linker increased from 0.25 wt% to 2.0 wt%, the water uptake decreased from 3710 ± 170 % to 1150 ± 160 %. Thus, the water uptake of GC/poly(EO-*co*-Gly) hydrogels cross-linked by 0.25 wt% poly(EO-*co*-Gly)-CHO was 3.5-fold higher than

that cross-linked by 2.0 wt% cross-linker. These results demonstrate that the hydrogel properties can be adjusted by simply varying the concentration of poly(EO-*co*-Gly)-CHO. In brief, increasing the cross-linker concentration causes a higher cross-linking density of the *in situ* fabricated hydrogels, resulting in shorter gelation times and a lower water uptake capacity.

3.3 Rheological characterization

The entire gelation process was conducted under physiological conditions (pH 7.4, 37 °C) and was monitored using a stress-controlled rheometer. Fig. 7A shows the changes of storage modulus (*G*') and loss modulus (*G*") as a function of time. At the beginning of the time sweep experiment, the *G′* value was higher than that of *G″,* indicating that the elastic component of the system dominates the viscous component. With increasing time, the *G*' increased rapidly and reached a plateau value within 900 s, indicating the completion of gelation *via* a Schiff's base reaction. However, the crossing point of *G*' and *G*", which is generally defined as the gel point in chemically cross-linked systems,[46] was not observed in the early stage of hydrogel formation due to rapid gelation. In fact, approximately 2 min is required for sample loading and parameter setting before launching of the rheological test.

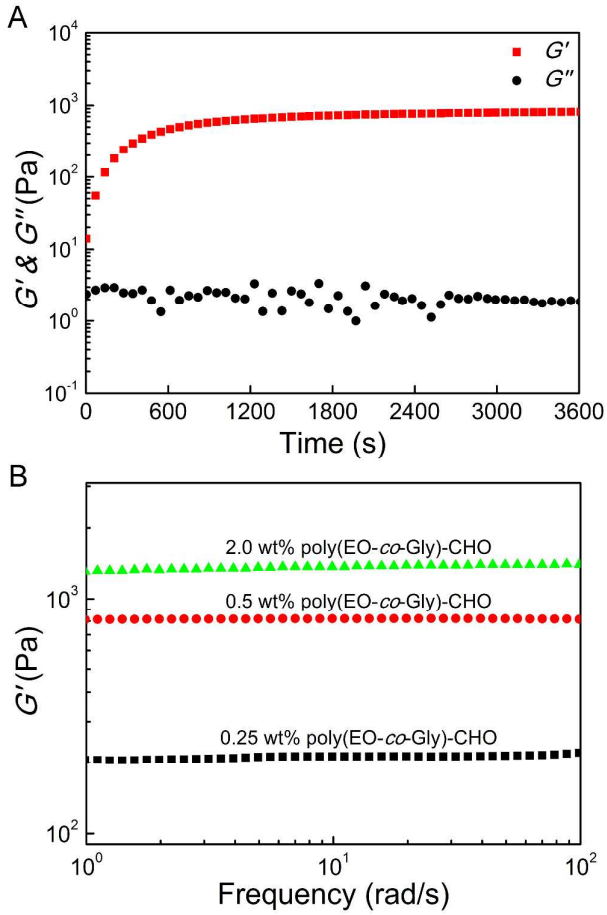

Fig. 7. (A) Time dependence of storage modulus (*G*') and loss modulus (*G*") of GC/poly(EO-*co*-Gly) hydrogels containing 1.5 wt% GC and 0.5 wt% poly(EO-*co*-Gly)-CHO at 37 °C. The oscillation frequency was set at 1 Hz. (B) *G*' of GC/poly(EO-*co*-Gly) hydrogels containing the indicated concentrations of poly(EO-*co*-Gly)-CHO as a function of frequency. The final concentration of GC in the hydrogel was fixed at 1.5 wt%. The test was initiated 2 h after sample loading with oscillation strain maintained at 1.0 % (corresponding to the LVER test).

The GC/poly(EO-*co*-Gly) hydrogels prepared using different concentrations of poly(EO-*co*-Gly)-CHO exhibited similar *G*' profiles in frequency sweep tests, as shown in Fig. 7B. Increasing the concentration of poly(EO-*co*-Gly)-CHO from 0.25

wt% to 2.0 wt% gave rise to a 7-fold increase in *G*' (210 vs. 1400 Pa). A *G*' of 800 Pa was obtained when the concentration of poly(EO-*co*-Gly)-CHO was set at 0.5 wt%. This finding suggests that the mechanical properties of *in situ* formed hydrogels were also well-manipulated by varying the cross-linker concentration. It has been widely recognized that the substrate stiffness of extracellular matrix (ECM) plays an important role in directing cellular processes including migration, proliferation and differentiation.[47, 48] As compared to two-dimensional substrates, cells experience a more sophisticated microenvironment in a three-dimensional system. Recently, it has been demonstrated chondrocyte functions are also stiffness-dependent in three-dimensional hydrogels.[49] Therefore, the ability to adjust hydrogel properties permits the possibility to modulate cellular functions in a three-dimensional ECM and facilitate a better understanding of the basic mechanisms of cell-ECM interaction.[6]

3.4 Hydrogel inner morphology

The inner morphology of GC/poly(EO-*co*-Gly) hydrogels was determined by SEM as presented in Fig. 8. SEM images show that the cross-section morphology and porosity of the hydrogel network were dependent on the content of poly(EO-*co*-Gly)-CHO. The porosity of the sponge structure tended to be more intact and uniform following an increase of concentration of poly(EO-*co*-Gly)-CHO from 0.25 wt% to 2.0 wt%. Furthermore, a porous inner morphology structure facilitates the migration of encapsulated cells and the efficient exchange of nutrients and metabolites.

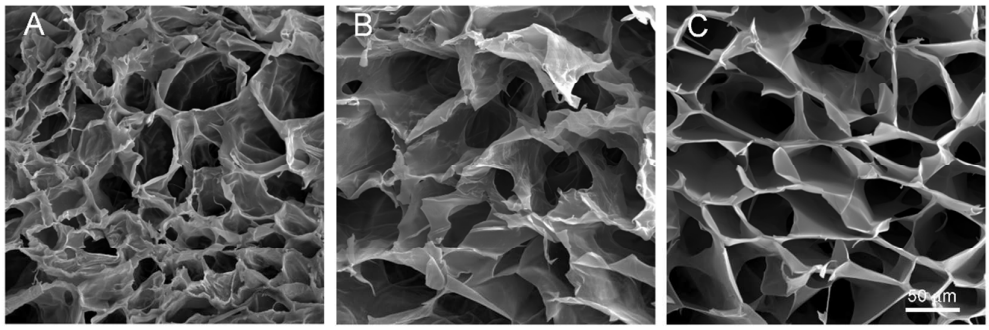

Fig. 8. Representative SEM images of freeze-dried GC/poly(EO-*co*-Gly) hydrogels containing various concentrations of poly(EO-*co*-Gly)-CHO: (A) 0.25 wt%, (B) 0.5 wt% and (C) 2.0 wt%. The final concentration of GC in the hydrogels was fixed at 1.5 wt%.

3.5 Hydrogel degradation *in vitro*

The biodegradation profile of tissue engineering scaffolds plays an important role in the reconstruction of specific tissues. The degradation of hydrogels could cause a change in the three-dimensional microenvironment, which in turn can affect motility and proliferation of encapsulated cells.[50] To evaluate the degradation profiles of GC/poly(EO-*co*-Gly) hydrogels, degradation testing was conducted *in vitro*. It is well-known that the glycosidic bonds of acetylated residues on the GC backbone can be enzymatically hydrolyzed by lysozyme.[35] To mimic degradation conditions *in vivo*, the hydrogels were incubated in PBS containing 1 mg/mL lysozyme, and the remaining gel was monitored as a function of time.

The results in Fig. 9 reveal that the concentration of poly(EO-*co*-Gly)-CHO had a significant effect on the degradation of GC/poly(EO-*co*-Gly) hydrogels. It is apparent that there was a gradual weight increase during the first 2 weeks for all of the

hydrogels, which was attributed to the increased water uptake after partial degradation of the hydrogels. Moreover, hydrogels prepared at a higher concentration of cross-linker exhibited a lower weight increase. This feature corresponds with the water uptake of hydrogels as shown in Fig. 6D. After 2 weeks, different degradation behaviors were observed for the GC/poly(EO-*co*-Gly) hydrogels prepared with different concentrations of cross-linker. Notably, the GC/poly(EO-*co*-Gly) hydrogels fabricated with 0.25 wt% and 0.5 wt% cross-linkers collapsed at 5 and 14 weeks post-incubation, respectively. In contrast, the GC/poly(EO-*co*-Gly) hydrogels containing 2.0 wt% cross-linker maintained their integrity even after incubating for 15 weeks.

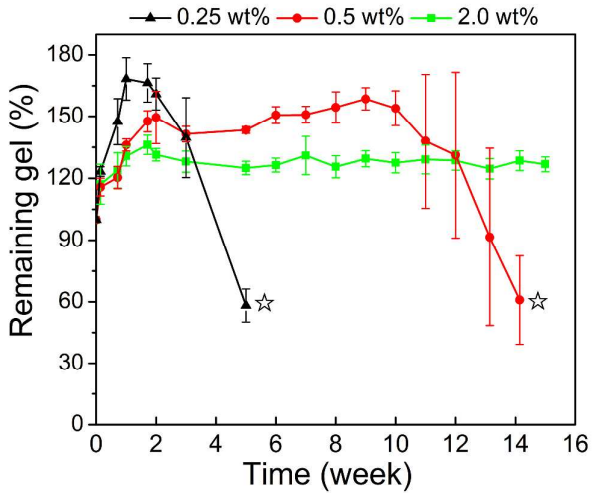

Fig. 9. *In vitro* degradation of GC/poly(EO-*co*-Gly) hydrogels fabricated with different concentrations of poly(EO-*co*-Gly)-CHO in PBS containing 1 mg/mL lysozyme at 37 °C. The final concentration of GC in the hydrogels was fixed at 1.5 wt%. "☆" indicates the collapse of hydrogels.

3.6 Hydrogel degradation *in vivo*

To further assess the degradation behaviors of hydrogels *in vivo*, we implanted the GC/poly(EO-*co*-Gly) hydrogels subcutaneously in the backs of ICR mice. An obvious elliptical protrusion appeared at the injection site, and a subsequent dissection revealed a transparent hydrogel that formed under the skin 30 min post-injection (Fig 10A).

All of the GC/poly(EO-*co*-Gly) hydrogels prepared with various concentrations of poly(EO-*co*-Gly)-CHO were allowed to develop over 12 weeks *in vivo*. The residual hydrogels were excised and recorded using a digital camera at predetermined time points (Fig. 10B). They were encapsulated by thin fibrous capsules and their sizes decreased gradually after being subcutaneously implanted in ICR mice. *In vivo* the degradation of the hydrogel appears to be governed by surface erosion, which can be attributed to an enzymatic hydrolysis of the GC segments. Meanwhile, the change in size *in vivo* was also dependent on the concentration of the cross-linker. For instance, the GC/poly(EO-*co*-Gly) hydrogels cross-linked with 0.25 wt% poly(EO-*co*-Gly)-CHO were almost completely degraded 12 weeks post-injection. As the poly(EO-*co*-Gly)-CHO concentration was increased to 0.5 wt% and 2.0 wt%, the residual hydrogels exhibited a relatively slower decrease in size compared with that formed at a lower concentration of cross-linker, such as 0.25 wt%. This indicates that these *in situ* formed hydrogels could serve as implantable biomaterials with adjustable

degradation profiles *in vivo*. Moreover, the long-term maintenance of the integrity of gels *in vivo* would allow the deposition of ECM before the gel degraded.

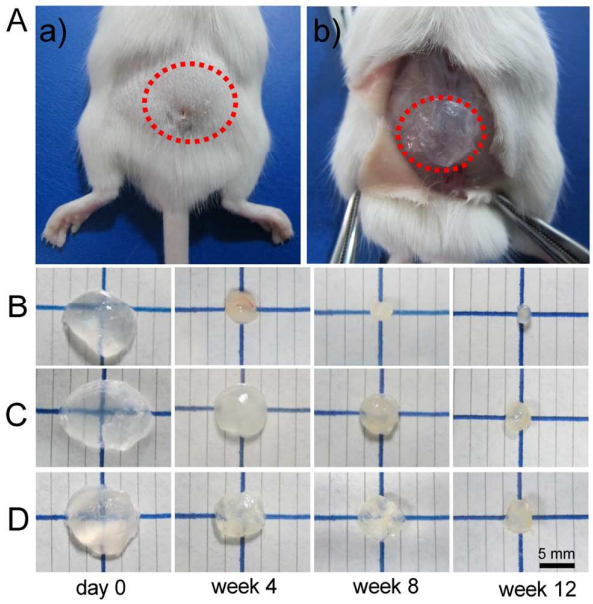

Fig. 10. (A) Global view after subcutaneous injection of the GC/poly(EO-*co*-Gly) hydrogel containing 0.5 wt% poly(EO-*co*-Gly)-CHO and 1.5 wt% GC into a ICR mouse (a), and subsequently dissection 30 min post-injection (b). The dashed circles indicate the presence of *in situ* formed hydrogels. (B-D) Photographs of the remaining hydrogels containing the indicated concentrations of poly(EO-*co*-Gly)-CHO: (B) 0.25 wt%, (C) 0.5 wt% and (D) 2.0 wt% removed from ICR mice after 0-12 weeks. The final concentration of GC in the hydrogels was fixed at 1.5 wt%.

It should be noted that the degradation behaviors of GC/poly(EO-*co*-Gly) hydrogels *in vitro* and *in vivo* displayed some differences. All of the hydrogels implanted subcutaneously in ICR mice maintained their integrity up to12 weeks, but the hydrogels fabricated with 0.25 wt% poly(EO-*co*-Gly)-CHO collapsed in PBS 5 weeks post-incubation. Because the physiological environment *in vivo* is more complex than

the degradation *in vitro*, such a difference would account for the different degradation behaviors.

3.7 Viability, proliferation and phenotype reservation of chondrocytes in the GC/poly(EO-*co*-Gly) hydrogels

Due to its avascular nature, adult articular cartilage has a very limited capability of self-healing once damaged.[51] To date, the regeneration of articular cartilage is still challenging in the clinic. The emergence of cartilage tissue engineering has shown great potential in the regeneration of cartilage defects. In this approach, a three-dimensional scaffold that functions as a temporary ECM is required to accommodate donor cells, which then can be implanted at the site of a cartilage defect.[52, 53] In this study, encapsulation of chondrocytes using GC/poly(EO-*co*-Gly) hydrogels was performed to evaluate their biological performance as an artificial ECM for cartilage tissue engineering.

Chondrocytes isolated from articular cartilage tissues from 7-day neonatal SD rats were successfully encapsulated in the GC/poly(EO-*co*-Gly) hydrogels containing 0.5 wt% poly(EO-*co*-Gly)-CHO and 1.5 wt% GC, as schematically illustrated in Fig. 11A. Then, the hydrogel/cell constructs were cultured in DMEM medium, and most of the chondrocytes were still viable 14 days post-encapsulation, as viewed using CLSM (Fig. 11B). Viable cells were stained with Calcein AM (green), and dead cells were stained with EthD-1 (red). The morphology of chondrocytes were also observed as a function of culture time. The fluorescence images in Fig. 11C reveal that elliptical or

round chondrocytes were homogenously distributed in the GC/poly(EO-*co*-Gly) hydrogels, and predominantly viable cells (greater than 90%) were found throughout the culture period. In addition, a formation of cell clusters was noted at day 14. These findings demonstrate that the gelation process does not compromise cell viability and that the GC/poly(EO-*co*-Gly) hydrogels exhibit excellent biocompatibility. Proliferation of the chondrocytes encapsulated in the hydrogels was also validated via a CCK-8 assay, as shown in Fig. 11D. The cell number decreased slightly 1 day post-encapsulation compared to that at day 0; however, there was no statistical difference. Interestingly, the cell number increased significantly during 14 days of culture, and there was a significant difference between day 1, day 7 and day 14. These results strongly suggest that the three–dimensional GC/poly(EO-*co*-Gly) gel matrix allows for sufficient transport of nutrients and oxygen to the encapsulated chondrocytes, resulting in cells that were highly viable and that proliferated effectively within the hydrogels.

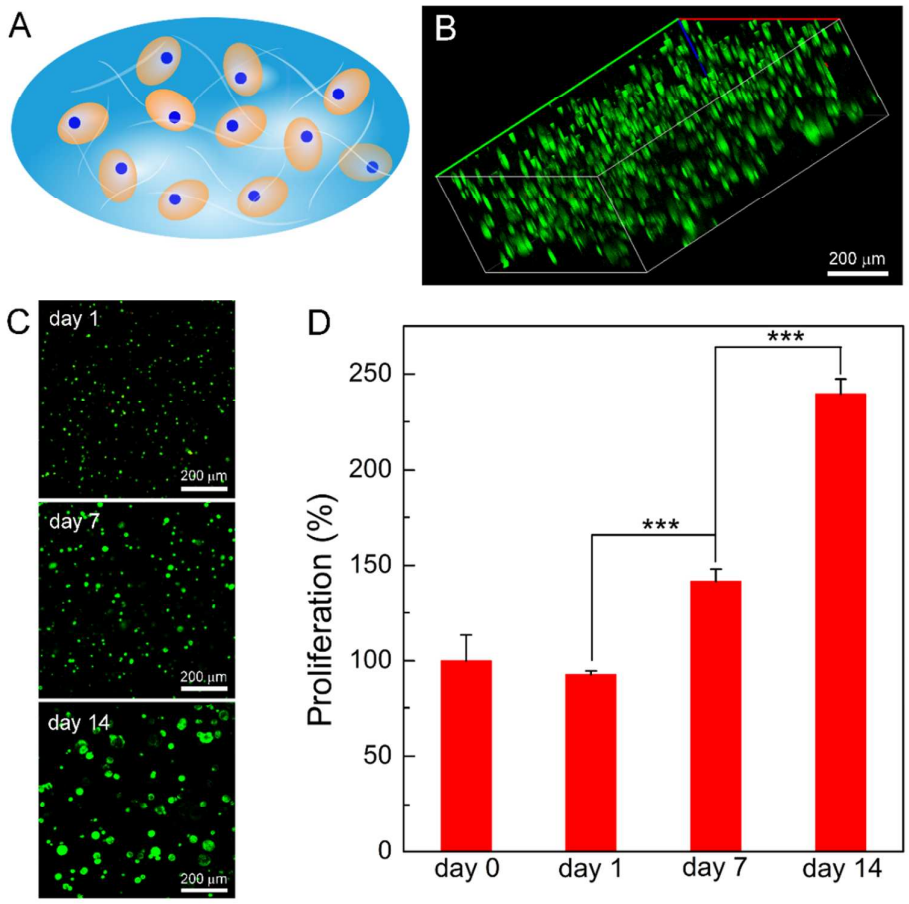

Fig. 11. (A) Schematic illustration of chondrocytes encapsulation in the GC/poly(EO-*co*-Gly) hydrogel. (B) Three-dimensional view of the hydrogel containing the chondrocytes 14 days post-encapsulation. Viable cells were stained with Calcein AM (green) and dead cells were stained with EthD-1 (red.); the cells were visualized using CLSM. Cell seeding density was 5×10^6 cells/mL. (C) Morphology of chondrocytes encapsulated in the GC/poly(EO-*co*-Gly) hydrogels after 1, 7 and 14 days of culture. (D) Proliferation of chondrocytes encapsulated in the GC/poly(EO-*co*-Gly) hydrogels after 1, 7 and 14 days of culture. All hydrogel samples contained 0.5 wt% poly(EO-*co*-Gly)-CHO and 1.5 wt% GC.

Unlike the round cell morphology observed for chondrocytes inside the hydrogels, chondrocytes cultured on traditional two-dimensional tissue culture plates (TCP) had a fibroblastic morphology, which is a sign of dedifferentiation, as shown in Fig. 12A. In fact, the development of cartilage tissue engineering has always suffered from the dilemma of dedifferentiation of chondrocytes during monolayer expansions *in vitro*.[54] As a result, the expression of collagen II, aggrecan and SOX9 decreased dramatically during successive passages of chondrocytes on two-dimensional TCP, indicating typical dedifferentiation of the chondrocyte phenotype,[55-57] and this phenomenon was also demonstrated in our experiments (Fig. 12B).

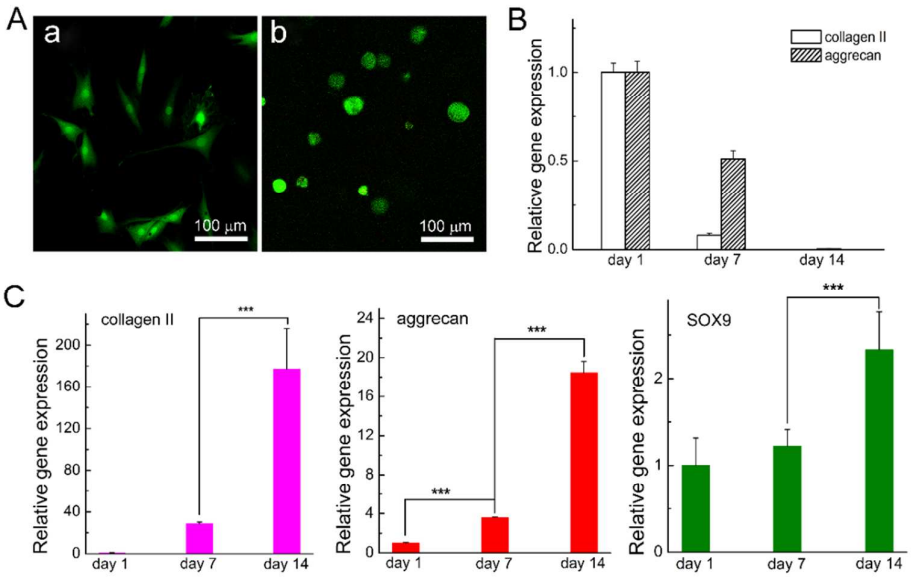

Fig. 12. (A) Morphology of chondrocytes passaged on TCPs (a) and in hydrogels (b) after 14 days of culture. The cells were stained and visualized using CLSM. While a fibroblast-like morphology and significant dedifferentiation of chondrocytes was observed after 14 days of culture on TCPs, chondrocytes exhibited a normal round morphology in the hydrogel matrix. (B) Relative gene expression of collagen II and

aggrecan of chondrocytes cultured on TCPs, confirming significant dedifferentiation on two-dimensional TCPs. (C) Relative gene expression of collagen II, aggrecan, SOX9 of encapsulated chondrocytes after 1, 7 and 14 days of culture, indicating the remaining of chondrocyte phenotype and the proliferation of chondrocytes in the three-dimensional hydrogels. Total RNA was extracted from the chondrocytes/hydrogel constructs at predetermined time points and the mRNA expression levels were determined by qRT-PCR measurements. All data are represented as the mean ± S.D (n = 4). "***" denotes $p < 0.001$. All hydrogel samples contained 0.5 wt% poly(EO-*co*-Gly)-CHO and 1.5 wt% GC.

Hence, preserving the phenotype of chondrocytes is a prerequisite for the regeneration of hyaline cartilage tissue with a long-term functionality. To examine the capability of phenotype reservation of embedded chondrocytes in hydrogels, the expression levels of characteristic genes were examined using qRT-PCR measurements. Considering the acid labile nature of the benzoic-imine bond,[29] the hydrogel/chondrocyte constructs were dissolved in acetic acid (3 wt%) to facilitate the extraction of total RNA. Three characteristic genes, including collagen II, aggrecan and SOX9, were detected. The results in Fig. 12C demonstrate that the expression of collagen II, aggrecan and SOX9 is up regulated at different levels. For example, the expression levels of collagen II of chondrocytes incorporated in hydrogels was significantly enhanced, being up regulated more than 170-fold at day 14 than that at day 1, and there was a significant difference between the relative expressions at day 7 and day 14. In the case of aggrecan, the relative expression was up regulated 18.5-fold

at day 14 compared with that at day 1, and there was a significant difference between every two time points. These results demonstrate that the three-dimensional hydrogel system in this study is beneficial to the preservation of the chondrocyte phenotype. In fact, our recent studies on two-dimensional micropatterned surfaces also illustrated that the round shape of chondrocytes is important to avoid dedifferentiation of chondrocytes during monolayer culture *in vitro*.[42] Consequently, our present study of chondrocytes in hydrogels is consistent with the previous findings of chondrocytes on two-dimensional surfaces.

4. Conclusion

A PEG analogue, poly(EO-*co*-Gly), containing multiple pendent hydroxyl groups was designed and synthesized by anionic random copolymerization of EO and EPEE with subsequent deprotection of the EPEE units. Next, functional benzaldehyde groups were successfully introduced into the poly(EO-*co*-Gly) copolymer, resulting in the formation of a novel multifunctional cross-linker, poly(EO-*co*-Gly)-CHO. Injectable hydrogels were conveniently *in situ* prepared by mixing a poly(EO-*co*-Gly)-CHO solution with a GC solution through the efficient and orthogonal formation of covalent benzoic-imine bonds under physiological conditions. The gelation time could be adjusted between 3.5 min to 1.0 min *via* increasing the concentration of poly(EO-*co*-Gly)-CHO. Both *in vitro* and *in vivo* testing confirmed the degradation of GC/poly(EO-*co*-Gly) hydrogels, and the life time of injected hydrogels *in vivo* was greater than 3 months. Chondrocytes encapsulated in

GC/poly(EO-*co*-Gly) hydrogels maintained a high viability and a round cell morphology after 14 days of three-dimensional culture. Further examination demonstrated that the cell proliferation was sustained and the phenotype of the chondrocytes was well preserved. These results demonstrate that the Schiff's base reaction provides a versatile platform for constructing injectable *in situ* hydrogels, and GC/poly(EO-*co*-Gly) hydrogels are promising biomaterials for cartilage tissue engineering.

Acknowledgement

The group was supported by the NSF of China (Grants No. 51273217, No. 91127028, and No. 21034002), the Chinese Ministry of Science and Technology (973 Program No. 2011CB606203) and the Science and Technology Developing Foundation of Shanghai (Grants No. 12JC1402600, No. 14441901500 and No. 13XD1401000).

References

1 D. Seliktar, *Science*, 2012, **336**, 1124-1128.
2 L. Yu and J. D. Ding, *Chem. Soc. Rev.*, 2008, **37**, 1473-1481.
3 J. A. Hunt, R. Chen, T. van Veen and N. Bryan, *J. Mater. Chem. B*, 2014, **2**, 5319-5338.
4 D. Y. Ko, U. P. Shinde, B. Yeon and B. Jeong, *Prog. Polym. Sci.*, 2013, **38**, 672-701.
5 D. A. Wang, S. Varghese, B. Sharma, I. Strehin, S. Fermanian, J. Gorham, D. H. Fairbrother, B. Cascio and J. H. Elisseeff, *Nat. Mater.*, 2007, **6**, 385-392.
6 X. Yao, R. Peng and J. D. Ding, *Adv. Mater.*, 2013, **25**, 5257-5286.
7 J. H. Jang, Y. M. Choi, Y. Y. Choi, M. K. Joo, M. H. Park, B. G. Choi, E. Y. Kang and B. Jeong, *J. Mater. Chem.*, 2011, **21**, 5484-5491.
8 B. G. Choi, M. H. Park, S. H. Cho, M. K. Joo, H. J. Oh, E. H. Kim, K. Park, D. K. Han and B. Jeong, *Biomaterials*, 2010, **31**, 9266-9272.
9 B. Yeon, M. H. Park, H. J. Moon, S. J. Kim, Y. W. Cheon and B. Jeong, *Biomacromolecules*, 2013, **14**, 3256-3266.

10 L. Yu, H. T. Hu, L. Chen, X. G. Bao, Y. Z. Li, L. Chen, G. H. Xu, X. J. Ye and J. D. Ding, *Biomater. Sci.*, 2014, **2**, 1100-1109.
11 R. Jin, L. S. Moreira Teixeira, P. J. Dijkstra, M. Karperien, C. A. van Blitterswijk, Z. Y. Zhong and J. Feijen, *Biomaterials*, 2009, **30**, 2544-2551.
12 J. S. Kwon, S. M. Yoon, D. Y. Kwon, D. Y. Kim, G. Z. Tai, L. M. Jin, B. Song, B. Lee, J. H. Kim, D. K. Han, B. H. Min and M. S. Kim, *J. Mater. Chem. B*, 2013, **1**, 3314-3321.
13 K. Li, L. Yu, X. J. Liu, C. Chen, Q. H. Chen and J. D. Ding, 2013, **34**, 2834-2842.
14 W. W. Wang, J. J. Liu, C. Li, J. Zhang, J. F. Liu, A. J. Dong and D. L. Kong, *J. Mater. Chem. B*, 2014, **2**, 4185-4192.
15 T. Y. Ci, L. Chen, L. Yu and J. D. Ding, *Sci. Rep.*, 2014, **4**, 5473.
16 L. Zeng, Y. Yao, D. A. Wang and X. Chen, *Mater. Sci. Eng. C. Mater. Biol. Appl.*, 2014, **34**, 168-175.
17 L. Yu, W. Xu, W. J. Shen, L. P. Cao, Y. Liu, Z. S. Li and J. D. Ding, *Acta Biomater.*, 2014, **10**, 1251-1258.
18 W. Leong, T. T. Lau and D. A. Wang, *Acta Biomater.*, 2013, **9**, 6459-6467.
19 J. M. Jukes, L. J. van der Aa, C. Hiemstra, T. van Veen, P. J. Dijkstra, Z. Zhong, J. Feijen, C. A. van Blitterswijk and J. de Boer, *Tissue. Eng. Part. A*, 2010, **16**, 565-573.
20 Y. Hong, H. Q. Song, Y. H. Gong, Z. W. Mao, C. Y. Gao and J. C. Shen, *Acta Biomater.*, 2007, **3**, 23-31.
21 L. Yu, K. Li, X. J. Liu, C. Chen, Y. C. Bao, T. Y. Ci, Q. H. Chen and J. D. Ding, *J. Pharm. Sci.*, 2013, **102**, 4140-4149.
22 H. P. Tan, C. R. Chu, K. A. Payne and K. G. Marra, *Biomaterials*, 2009, **30**, 2499-2506.
23 R. Jin, L. S. Moreira Teixeira, A. Krouwels, P. J. Dijkstra, C. A. van Blitterswijk, M. Karperien and J. Feijen, *Acta Biomater.*, 2010, **6**, 1968-1977.
24 G. T. Chang, T. Y. Ci, L. Yu and J. D. Ding, *J. Control. Release.*, 2011, **156**, 21-27.
25 B. G. Choi, M. H. Park, S. H. Cho, M. K. Joo, H. J. Oh, E. H. Kim, K. Park, D. K. Han and B. Jeong, *Soft Matter*, 2011, **7**, 456-462.
26 F. Yang, J. Wang, L. Y. Cao, R. Chen, L. J. Tang and C. S. Liu, *J. Mater. Chem. B*, 2014, **2**, 295-304.
27 N. E. Fedorovich, M. H. Oudshoorn, D. van Geemen, W. E. Hennink, J. Alblas and W. J. Dhert, *Biomaterials*, 2009, **30**, 344-353.
28 D. Steinhilber, S. Seiffert, J. A. Heyman, F. Paulus, D. A. Weitz and R. Haag, *Biomaterials*, 2011, **32**, 1311-1316.
29 C. X. Ding, L. L. Zhao, F. Y. Liu, J. Cheng, J. X. Gu, D. Shan, C. Y. Liu, X. Z. Qu and Z. Z. Yang, *Biomacromolecules*, 2010, **11**, 1043-1051.
30 Y. Xin and J. Y. Yuan, *Polym. Chem.*, 2012, **3**, 3045-3055.
31 Y. Zhang, L. Tao, S. Li and Y. Wei, *Biomacromolecules*, 2011, **12**, 2894-2901.
32 B. Balakrishnan, N. Joshi and R. Banerjee, *J. Mater. Chem. B*, 2013, **1**, 5564-5577.
33 J. Berger, M. Reist, J. M. Mayer, O. Felt, N. A. Peppas and R. Gurny, *Eur. J. Pharm. Biopharm.*, 2004, **57**, 19-34.
34 B. Balakrishnan and A. Jayakrishnan, *Biomaterials*, 2005, **26**, 3941-3951.
35 L. Li, N. Wang, X. Jin, R. Deng, S. H. Nie, L. Sun, Q. Wu, Y. Q. Wei and C. Y. Gong, *Biomaterials*, 2014, **35**, 3903-3917.
36 K. Y. Lee, E. Alsberg and D. J. Mooney, *J. Biomed. Mater. Res. Part A*, 2001, **56**, 228-233.
37 A. O. Fitton, J. Hill, D. E. Jane and R. Millar, *Synthesis*, 1987, 1140-1142.
38 Z. Y. Li, P. P. Li and J. L. Huang, *J. Polym. Sci. Part A: Polym. Chem.*, 2006, **44**, 4361-4371.

39 A. Postma, T. P. Davis, A. R. Donovan, G. X. Li, G. Moad, R. Mulder and M. S. O'Shea, *Polymer*, 2006, **47**, 1899-1911.
40 L. Yu, T. Y. Ci, S. C. Zhou, W. J. Zeng and J. D. Ding, *Biomater. Sci.*, 2013, **1**, 411-420.
41 C. Chen, L. Chen, L. P. Cao, W. J. Shen, L. Yu and J. D. Ding, *RSC. Adv.*, 2014, **4**, 8789-8798.
42 B. Cao, R. Peng, Z. H. Li and J. D. Ding, *Biomaterials*, 2014, **35**, 6871-6881.
43 H. C. Patschureck, E. Edmans and J. Bennett, *Abstr. Pap. Am. Chem. Soc.*, 2013, **245**
44 V. W. Goodlett, *Anal. Chem.*, 1965, **37**, 431-&.
45 Z. Li, S. Cho, I. C. Kwon, M. M. Janat-Amsbury and K. M. Huh, *Carbohydr. Polym.*, 2013, **92**, 2267-2275.
46 F. Lin, J. Y. Yu, W. Tang, J. K. Zheng, A. Defante, K. Guo, C. Wesdemiotis and M. L. Becker, *Biomacromolecules*, 2013, **14**, 3749-3758.
47 C. M. Kirschner, D. L. Alge, S. T. Gould and K. S. Anseth, *Adv. Healthc. Mater.*, 2014, **3**, 649-657.
48 T. P. Appelman, J. Mizrahi, J. H. Elisseeff and D. Seliktar, *Biomaterials*, 2009, **30**, 518-525.
49 L. S. Wang, C. Du, W. S. Toh, A. C. Wan, S. J. Gao and M. Kurisawa, *Biomaterials*, 2014, **35**, 2207-2217.
50 D. D. McKinnon, D. W. Domaille, J. N. Cha and K. S. Anseth, *Adv. Mater.*, 2014, **26**, 865-872.
51 M. Keeney, J. H. Lai and F. Yang, *Curr. Opin. Biotechnol.*, 2011, **22**, 734-740.
52 P. G. Duan, Z. Pan, L. Cao, Y. He, H. R. Wang, Z. H. Qu, J. Dong and J. D. Ding, *J. Biomed. Mater. Res. Part A*, 2014, **102**, 180-192.
53 J. W. Chen, C. Y. Wang, S. H. Lu, J. Z. Wu, X. M. Guo, C. M. Duan, L. Z. Dong, Y. Song, J. C. Zhang, D. Y. Jing, L. B. Wu, J. D. Ding and D. X. Li, *Cell. Tissue. Res.*, 2005, **319**, 429-438.
54 T. Hoshiba, H. X. Lu, N. Kawazoe, T. Yamada and G. P. Chen, *Biotechnol. Prog.*, 2013, **29**, 1331-1336.
55 M. Gosset, F. Berenbaum, S. Thirion and C. Jacques, *Nat. Protoc.*, 2008, **3**, 1253-1260.
56 E. M. Darling and K. A. Athanasiou, *J. Orthop. Res.*, 2005, **23**, 425-432.
57 M. J. Wozniak, N. Kawazoe, T. Tateishi and G. P. Chen, *Soft Matter*, 2010, **6**, 2462-2469.

Graphical and textual abstract for TOC

An injectable hydrogel formed by *in situ* cross-linking of glycol chitosan and multi-benzaldehyde functionalized PEG analogues for cartilage tissue engineering

Luping Cao, Bin Cao, Chengjiao Lu, Guowei Wang, Lin Yu, Jiandong Ding*

A novel PEG analogue, poly(EO-*co*-Gly)-CHO, that possesses multiple aldehyde groups is designed and synthesized, and then is used as a cross-linker to react with glycol chitosan through Schiff's base reaction to create injectable hydrogels under physiological conditions.